THE RELATIVE CONTRIBUTIONS OF THE FOLDS AND CAVEOLAE TO THE SURFACE MEMBRANE OF FROG SKELETAL MUSCLE FIBRES AT DIFFERENT SARCOMERE LENGTHS

By ANGELA F. DULHUNTY* AND
CLARA FRANZINI-ARMSTRONG†

*From the Department of Physiology, University of Rochester,
Rochester, N.Y. 14642, U.S.A.*

SUMMARY

The plasmalemmal area of striated muscle fibres is greater than the apparent surface area (A = circumference × length) because of variable folds and the invaginations of the caveolae and T-tubules. Freeze-fracture replicas of the surface membrane of sartorius and semitendinosus muscles from *Rana pipiens* have been used to determine the numbers and distribution of folds and caveolae at different sarcomere lengths.

(1) The plasmalemma folds are variable in size and shape, but are always oriented perpendicular to the long axis of the fibre. The folds vary with stretch, being more prominent at short sarcomere lengths. The caveolae are elliptical invaginations of the plasmalemma which open to the outside by a narrow 'neck' of approximately 20 nm. The caveolar lumen has an average long dimension of 81·6 ± 11·7 nm and an average short dimension of 66·9 ± 7·9 nm. The caveolar 'necks' only can be seen in freeze-fracture replicas and these are distributed in two circumferential bands on either side of the Z-line, and in longitudinal bands separated by distances of 1–5 μm. In the sartorius muscle, at a sarcomere length of 2·8 μm, there is an average number of thirty-seven caveolae per square micrometer of fibre surface.

(2) During passive stretch the opening of folds provides membrane for the necessary increase in surface area up to a sarcomere length of about 3·0 μm. This length is defined as the critical sarcomere length (S_c). The number of caveolae remains constant at all sarcomere lengths

* Present address: School of Life Sciences, N.S.W. Institute of Technology, Australia 2007.

† Present address: Department of Biology, University of Pennsylvania, Philadelphia, Penn. 19104, U.S.A.

less than S_c and thus their 'necks' have been used as membrane markers to determine the amount of folding at different sarcomere lengths. The membrane area contained in folds and caveolae is expressed as a fraction of the apparent surface area (A). For example, in the sartorius muscle, at a sarcomere length of 2·4 μm, the membrane area, excluding the T-tubules, is:

$$A + 0·1A \text{ (folding)} + 0·7A \text{ (caveolae)} = 1·8A.$$

(3) For stretch beyond S_c membrane is provided by the opening of caveolae. At a sarcomere length of about 8 μm all the caveolae are open and the fibres rupture with further stretch.

(4) The relative contributions of folds and caveolae vary with sarcomere length in a way that is consistent with assumptions of constant volume and plasmalemma area. The maintenance of constant plasmalemma area, even after excessive stretch, suggests that the plasmalemma is relatively inelastic in this situation.

INTRODUCTION

Physiological properties of the surface membrane of muscle fibres are often quoted in units of membrane area. The area of membrane cannot be measured directly and is usually calculated from measurements of one or two diameters of the fibre with the assumption that the fibre has a smooth circular or elliptical outline. This approach can lead to significant errors (Blinks, 1965; Dulhunty & Gage, 1973). A particular example of the importance of membrane area can be found in the numerous electrophysiological studies of amphibian skeletal muscle fibres. It is well known that the specific electrical properties of muscle differ in a characteristic way from those of nerve (Katz, 1948). This difference can, in part, be explained on geometrical grounds (Falk & Fatt, 1964; Gage & Eisenberg, 1969) and so it is important to have an accurate definition of the outline of the muscle fibre, including membrane folding and membrane systems that are continuous with the surface membrane. One of these is the transverse tubular (T) system (Andersson-Cedergren, 1959) and its contribution to the total surface area of frog and toad twitch and slow muscle fibres has been determined (Page, 1964; Peachey, 1965; Peachey & Schild, 1968; Eisenberg, 1972). Other surface invaginations, the caveolae (Bennett, 1960; Rayns, Simpson & Bertaud, 1968; Franzini-Armstrong, 1973; Zampighi, Vergara & Ramón, 1974), have attracted less attention, even though they are numerous and must contribute to the mechanical and electrical properties of the plasmalemma (Rayns et al. 1968; Dulhunty & Gage, 1973).

This investigation was initiated with the purpose of obtaining a

quantitative definition of the contribution of the caveolae and of folding to the total plasmalemmal area. We were also interested in the extent to which the caveolae might function as a reservoir of membrane to be recruited during stretch. We have used freeze-fracture, which allows examination of large areas of the plasmalemma, and is well suited to a study of the number and distribution of caveolar openings at the fibre's surface.

From the results it is possible to determine the contribution of surface folds and caveolae to the surface area of a fibre and to show that the total membrane area is constant at all sarcomere lengths. The same general conclusions have been concomitantly reached using thin sections (Peachey & Terrell, 1974). Thus we have a unique situation in which the total plasmalemmal area of a fibre can be accurately defined once the (fibre) cross-section and sarcomere length are known.

TABLE 1. Fibre diameter measured from eighteen isolated fibres during fixation and glycerol infiltration (% unfixed fibre diameter)

	Glutaraldehyde 3·5%	Glycerol 5%	Glycerol 10%	Glycerol 20%	Glycerol 30%
Mean	98·8	98·9	96·8	96·8	96·4
± 1 S.E. of mean	1·0	0·9	0·8	0·8	0·9

METHODS

Sartorius and semitendinosus muscles from *Rana pipiens* were used. The muscles were tied to a holder and stretched to the required length before fixation. It is well known that sartorius muscles cannot be stretched to sarcomere lengths greater than 2·8 μm and thus semitendinosus muscles were used for experiments requiring greater stretch.

Thin sections. Muscles were fixed in 3·5% glutaraldehyde (0·1 M cacodylate or phosphate buffer, pH = 7·2, for 1–2 hr at room temperature), washed in buffer and post-fixed in 2% OsO_4 in the same buffer. This was followed by dehydration in ethanol and embedding in Epon, 812.

Freeze-fracture. The muscles were fixed in 3·5% glutaraldehyde, as above, and then gradually infiltrated with 5, 10, 15, 20 and 30% solutions of glycerol in water. Twenty minutes equilibration in each solution, at room temperature, was allowed. The amount of shrinkage following this treatment was measured in eighteen isolated semitendinosus fibres and the results are listed in Table 1. The diameters of the fibres were measured with a calibrated eyepiece micrometer in a light microscope and are expressed as a percentage of the diameter measured in normal Ringer solution before fixation(Table 1). Measurements were made after 60 min in the fixative (column 1) and then after 20 min in four of the glycerol solutions (columns 2, 3, 4 and 5). After final equilibration in 30% glycerol the average diameter was 3·6% less than the control. Additional data were obtained from optical sections of isolated fibres (cf. Blinks, 1965) measured throughout an identical series of solution changes. Table 2 lists the results of three fibres; the

cross-section was measured with a planimeter and the circumference measured with a map measuring device. There is an average 4·4 % reduction in the circumference and a 10 % reduction in the cross-sectional area.

Fracturing and shadowing were done in a Denton DFE-3 Freeze etch unit (Denton Vacuum, Inc., Cherry Hill, New Jersey) mounted on a Kinney (KSE-2A-M) evaporator (Kinney Vacuum Co., Boston, Massachusetts). Pictures were taken in an AEI 801 electron microscope at standardized magnifications.

Determination of sarcomere length. The results are invariably expressed as a function of sarcomere length and therefore we took precautions to ensure that the measurement of sarcomere length was as accurate as possible. The sarcomere length was measured from the muscle after fixation and glycerol infiltration. The measurement was made either with a calibrated eyepiece micrometer in a light microscope at a magnification of 1000 ×, or by laser beam diffraction. Another area of the same muscle was then used for freeze-fracture. In the freeze-fracture replica the plasma membrane is always slightly indented along the Z-line and so the sarcomere length could be measured on each fibre counted for the numerical analysis. In the sartorius muscle the fibres have a uniform sarcomere length throughout the muscle and the two sets of measurements could be directly compared. The sarcomere length measured after freeze-fracture was generally shorter than that measured in the light microscope although the difference was normally less than 0·2 μm.

TABLE 2. Circumference and cross-section measured from optical sections of three isolated fibres during fixation and glycerol infiltration (% unfixed fibre dimension)

	Fibre	Glutar-aldehyde 3·5 %	Glycerol 5 %	Glycerol 10 %	Glycerol 20 %	Glycerol 30 %
Circumference	1	96	99	94	97	97
	2	95	95	98	93	93
	3	95	95	99	97	97
Cross-section	1	94	90	85	95	93
	2	94	90	95	86	86
	3	92	88	96	92	90

The semitendinosus is more complex. The fibres have different lengths depending on their attachment to the tendon and longer fibres have shorter sarcomere lengths. When the muscle is fixed *in situ*, with the knee bent at 90°, the range of sarcomere lengths is 2·9–3·2 μm. Thus the 'resting sarcomere length' in the semitendinosus is much longer than that in the sartorius muscle which is frequently reported in the literature as 2·2 μm. The difference in sarcomere lengths in a semitendinosus muscle is magnified with stretch; for example, when the average sarcomere length is 5·0 μm, the range of sarcomere lengths is 1·0 μm.

Statistically, muscles fixed at short lengths gave more accurate results because fibres had fairly uniform sarcomere lengths within each fractured bundle and thus average results could be obtained from a number of fibres. In stretched muscles, the probability of finding two fibres with identical sarcomere lengths became very low and the data had to be tabulated separately.

Constant volume equations

In order to analyse the data we used a set of equations that assume constant volume and define the relationship between fibre diameter, surface area and sarcomere length. For a circular cylinder of length S and radius r,

$$r = \sqrt{\frac{\text{vol.}}{\pi S}}. \qquad (1)$$

The surface area,

$$A = 2\pi r S. \qquad (2)$$

For two cylinders with the same volume, but different lengths, S and S', the radii, r and r' are related as follows:

$$\frac{r}{r'} = \sqrt{\frac{S'}{S}}. \qquad (3)$$

The surface areas, A and A', must also vary if the volume is to remain constant.

$$\frac{A}{A'} = \frac{2\pi r S}{2\pi r' S'}. \qquad (4)$$

Inserting eqn. (3),

$$\frac{A}{A'} = \sqrt{\left(\frac{S'}{S}\right) \cdot \frac{S}{S'}} = \sqrt{\frac{S}{S'}}. \qquad (5)$$

Fractional area of folds and caveolae

The aim of this study is to find out how estimates of membrane area, based on calculations of the apparent surface area (i.e. circumference × length), are altered by the presence of folds and caveolae. One approach is to calculate the relative areas of membrane in the two structures and to express these as fractions of a unit area of the apparent surface of the fibre. Intuitively both fractions must decrease as the fibre lengthens.

Working hypothesis

Assumptions

(i) The fibres maintain constant volume at all sarcomere lengths.

(ii) The total plasmalemma area of the fibre (i.e. apparent surface area plus areas 'concealed' in folds and caveolae) is constant.

(iii) The number of caveolar necks per sarcomere remain constant at sarcomere lengths less than a critical sarcomere length.

(iv) The area of caveolar plasmalemma associated with each caveolar neck is a constant and independent of sarcomere length, i.e. it remains constant whether the caveolae are in the neck structure, or present as domes, or flattened.

(v) Non-caveolar plasmalemma is constant at sarcomere lengths less than the critical sarcomere length.

Table 3 has been constructed to define parameters used in the working hypothesis and emphasize differences between actual values (per sarcomere) and normalized values (per unit area of apparent surface). The Table shows how each parameter varies with sarcomere length. Four sarcomere lengths are defined: (1) S_c, the critical sarcomere length, at S_c the plasmalemma has unfolded, but the caveolae have not opened; (2) S_o, the sarcomere length at which all the caveolae have opened and flattened; (3) S_1, any sarcomere length less than S_c; (4) S_2, any sarcomere length between S_c and S_o.

For establishing the working hypothesis, we assume that each parameter defined in Table 3 varies with sarcomere length in such a way as to maintain constant volume and constant total plasmalemma area (see Assumptions). (In the Results section we measured the number of caveolar necks per sarcomere, n, and the number per unit area of apparent surface, N. From these numbers we could determine the true area of caveolar membrane, β, and the area of folding, α, over a range of sarcomere lengths. Thus we could compare experimentally determined values with those predicted by the working hypothesis.)

Actual values

The first section of Table 1 defines actual values (per sarcomere). These will not be used later but are essential in the derivation of the normalized values.

The constant volume equations (see eqns. 1–5) show that the apparent surface area, A, of a cylinder of length S, increases as S increases and is proportional to $\sqrt{S}$. Using the subscripts of Table 3, eqn. 5 can be written as:

$$\frac{A_1}{A_2} = \sqrt{\frac{S_1}{S_2}}. \tag{6}$$

Since A increases with S, but the total plasmalemma remains constant, extra membrane must be available to be recruited during stretch. We assume that the extra membrane is contained in the folds and caveolae. Folding provides membrane for stretch up to the critical sarcomere length and the caveolae opening provides membrane for stretch to greater lengths.

The number of caveolar necks, n, is used to indicate the membrane contained in caveolar plasmalemma. Incorporation of caveolar plasmalemma into non-caveolar plasmalemma is seen by a reduction in the number of caveolar necks. Thus for $S_1 < S_c$, n_1 is a constant. For $S_2 > S_c$, n_2 decreases by a fraction, γ, which is the fraction of necks 'lost' as the caveolae open. At S_0 all the caveolae have opened and $\gamma = 1$. The area of caveolar plasmalemma, J, is proportional to n. To obtain values of J the average plasmalemmal area of one caveola, c, was measured from thin sections. It will be shown later that each caveolar neck is the surface representation of two caveolae. Thus $J = 2nc$. For $S_1 < S_c$, the number of caveolae, and thus the caveolar plasmalemma, is a constant. For $S_2 > S_c$, the caveolar plasmalemma is reduced by the number of necks lost, i.e. by γ.

The area of non-caveolar plasmalemma, Q, is a constant for $S_1 < S_c$. The plasmalemma is thrown into folds so as to maintain constant volume as the fibre shortens. The area of non-caveolar plasmalemma, in this range, is defined as: $Q_1 = A_1(1+\alpha)$, where α is the fraction of plasmalemma contained in folds. At S_c the non-caveolar plasmalemma is unfolded and $Q_c = A_c$. At longer sarcomere lengths, $S_2 > S_c$, the non-caveolar plasmalemma is increased by addition of plasmalemma from the caveolae and $Q_2 = A_2 = A_c + 2n\gamma c$.

Normalized values

The second section of Table 3 shows how the normalized values (per unit area of apparent surface) are derived from the actual values and shows how each of the normalized values varies with sarcomere length.

The number of necks (per unit area of apparent surface), N, decreases with increasing sarcomere length. When $S_1 < S_c$, the decrease is proportional to unfolding of non-caveolar plasmalemma. When $S_2 > S_c$ the decrease is due to caveolae becoming domes (i.e. to an increase in γ). The variation of N with S can be

TABLE 3. Summary of working hypothesis (* symbols marked with an asterisk are defined at the end of the table)

	S_1		S_c		S_2		S_o
S Sarcomere length	S_1	<	S_c	<	S_2	<	S_o
Actual values (per sarcomere)							
A Apparent surface area (i.e. cylinder of length S)	A_1	<	A_c	<	A_2	<	A_o
n Number of necks	n_1	=	n_c	>	n_2 [$n_1(1-\gamma^*)$]	>	zero ($\gamma = 1$)
J* Area of caveolar plasmalemma	J_1 [$2n_1c^*$]	=	J_c [$2n_1c$]	>	J_2 [$2n_1(1-\gamma)c$]	>	zero
Q Area of non-caveolar plasmalemma	Q_1 [$A_1(1+\alpha^*)$]	<	Q_c [A_c]	<	Q_2 [$A_2 = A_c + 2n\gamma c$]	<	Q_o [$A_o = A_c + 2nc$]
Normalized values (per unit area of apparent surface)							
N = (n/A) Number of necks	N_1	>	N_c	>	N_2	>	zero
β = (J/A) Fractional area of caveolar plasmalemma	β_1	>	β_c	>	β_2	>	zero
P = (Q/A) Fractional area of non-caveolar plasmalemma	P_1 (1+α)	>	P_c (1)	=	P_2 (1)	=	P_o (1)
TP = Total plasmalemmal area per sarcomere	TP_1	>	TP_c	=	TP_2	=	TP_o
TP = A(P+β)	[$A_1(1+\alpha+\beta_1)$]	>	[$A_c(1+\beta_c)$]	=	[$A_2(1+\beta_2)$]	=	[A_o]
M = (TP/A) Total plasmalemma per unit area	M_1 $(1+\alpha_1+\beta_1)$	>	M_c $(1+\beta_c)$	>	M_2 $(1+\beta_2)$	>	M_o (1)

* (i) γ = fraction of necks 'lost', due to caveolae becoming domes and flattening.
(ii) c = average plasmalemma area of one caveola.
(iii) J = $2c$ × number of necks (see text for explanation).
(iv) α = folded plasmalemma, expressed as a fraction of apparent surface area.

predicted, for $S_1 < S_c$, using the constant volume equations. The normalized number of necks is defined as $N = n/A$. The ratio of N_1 and N_c is

$$\frac{N_1}{N_c} = \frac{A_c}{A_1} \cdot \frac{n_1}{n_c}. \tag{7}$$

Since we use the specific assumption that, for $S_1 < S_c$, $n_1 = n_c$, eqn. 6 can be written as:

$$\frac{N_1}{N_c} = \frac{A}{A_1}, \tag{8}$$

and from eqn. 6:

$$\frac{N_1}{N_c} = \sqrt{\frac{S_c}{S_1}}. \tag{9}$$

For $S_2 > S_c$, $n_2 \neq n_c$ and predictions of N_2 would require specific assumptions about the variation of γ with sarcomere length. This will be dealt with later (see p. 529).

The area of caveolar plasmalemma (per unit area of apparent surface), β, also decreases with sarcomere length. Specific predictions can be made about the behaviour of β_1 with changes in sarcomere length. For $S_1 < S_c$, β_1 is defined as:

$$\beta_1 = \frac{J_1}{A_1} = \frac{2n_1 c}{A_1}.$$

The ratio of β_1 to β_c is:

$$\frac{\beta_1}{\beta_c} = \frac{A_c}{A_1} \cdot \frac{2n_1 c}{2n_1 c}. \tag{10}$$

Therefore

$$\frac{\beta_1}{\beta_c} = \frac{A_c}{A_1} = \sqrt{\frac{S_c}{S_1}}. \tag{11}$$

The non-caveolar plasmalemma, expressed per unit of apparent surface, P, decreases as S_1 approaches S_c. The reduction in P is due to unfolding of the plasmalemma. When $S_2 > S_c$, the non-caveolar plasmalemma is flat and thus its area, per unit area of apparent surface does not vary, i.e. $P_c = P_2 = P_o = 1$. From the definitions in Table 3, $P = Q/A$ and the ratio P_1 to P_c is:

$$\frac{P_1}{P_c} = \frac{Q_1}{Q_c} \cdot \frac{A_c}{A_1}. \tag{12}$$

For $S_1 < S_c$, $Q_1 = Q_c$ and thus

$$\frac{P_1}{P_c} = \frac{A_c}{A_1}. \tag{13}$$

From eqn. 6

$$\frac{P_1}{P_c} = \sqrt{\frac{S_c}{S_1}}. \tag{14}$$

From the relationship shown in eqn. 14 we can derive a relationship between sarcomere length and plasmalemma folding. From Table 3, $P_1 = 1 + \alpha$ for $S_1 < S_c$. When $S_1 = S_c$, $P_c = 1$. Thus

$$\frac{1 + \alpha}{1} = \frac{P_1}{P_c} = \sqrt{\frac{S_c}{S_1}}, \tag{15}$$

$$\alpha = \sqrt{\frac{S_c}{S_1}} - 1. \tag{16}$$

<div align="center">RESULTS</div>

<div align="center">*General description*</div>

The structure of the plasmalemma and caveolae

The plasmalemma forms folds, of variable size and shape, mostly oriented circumferentially to the fibre (Pl. 1). The folds vary with stretch, being more prominent at short sarcomere lengths as is obvious in Pls. 1, 2. The critical sarcomere length (S_c) of the fibre is defined as the sarcomere length at which no folds are present on the surface of the fibre, i.e. the plasmalemma envelope is smooth. A freeze-fracture replica of a fibre near S_c is shown in Pl. 2. The caveolae are small in-pocketings of the plasma membrane, approximately elliptical, which open to the outside by a narrow neck with an opening of approximately 20 nm (C. Franzini-Armstrong, L. Landmesser & G. Pilar, to be published; Zampighi *et al.* 1974). The caveolar openings are shown in Pl. 3*A*, *B*.
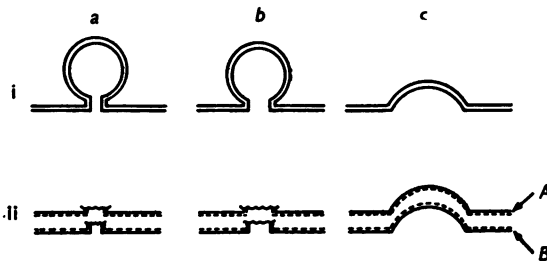
Text-fig. 1. A schematic diagram of the three structural states of the caveolae, (i)*a*, *b*, and *c*, and the way in which each of these is split during freeze fracture, (ii)*a*, *b*, and *c*. The extracellular space is below the membrane in both cases. The caveolae normally have a neck structure, (i)*a* and *b*, which is too sharp for the fracture plane to follow and which breaks as illustrated in (ii)*a* and *b*. On Face *A*, the neck structure will appear indented and on Face *B*, it will appear raised. When the caveolae have a dome structure, (i)*c*, the fracture follows their membrane, (ii)*c*. The domes are concave on the internal leaflet, (*A*), and convex on the external leaflet, (*B*).

In freeze-fracture, the fracture plane preferentially follows the interior of the membrane (Pinto da Silva & Branton, 1970; Tillack & Marchesi, 1970) which thus separates into two leaflets, a cytoplasmic leaflet, whose exposed fracture face is called Face *A*, and an exterior leaflet whose face is called Face *B*.

At the sites of attachment of the caveolae the plasmalemma turns sharply and the fracture plane follows the membrane only for a short distance into the neck. This is illustrated schematically in Text-fig. 1*a*.

The caveolae openings thus appear as circular indentations on Face A (Pl. 4 A) and as raised circles on Face B (Pl. 4 B). The circles will be referred to as 'necks' on both faces. In general necks could be more easily identified on Face B and this was used for numerical analysis wherever possible. The size of the necks was always measured in a direction perpendicular to the shadow. The average diameter of 196 necks is $34·3 \pm 2·3$ nm (mean ± 1 s.e. of mean). Theoretically the external diameter of the necks, seen on the fracture faces should equal the sum of the diameter of the caveolar opening as measured in sections, plus the width of two half membranes (see Text-fig. 1a), i.e. approximately 27·5 nm. The actual measurement is significantly larger. One possible reason is that the neck diameter was measured at the narrowest point in sections, but may not break at that point in freeze-fracture. Alternatively, it may simply be due to differences in preparative procedures. A small number of caveolae (less than 10%) have larger necks, up to 70 nm (Text-fig. 1b).

As fibres are stretched to sarcomere lengths longer than $3·2 \mu m$ the caveolae open and flatten into the plane of the plasmalemma. As the caveolae open the indentation of the neck becomes less sharp and the fracture plane follows the membrane without interruption (Text-fig. 1). The resulting structure will be referred to as a 'dome' (Pl. 4 C). When the caveolar membrane is thus exposed and almost flat, it appears free of particles on both fractured faces, in marked contrast to the rest of the membrane which contains a large number of particles, particularly on Face A (see Pl. 4 A and C).

In the final stage of opening, the membrane of the caveolae is completely flat and thus it forms a part of the surface membrane (Pl. 4 C). At that stage most of the caveolae can still be identified because their membrane remains free of particles on both fracture faces (Dulhunty & Franzini-Armstrong, 1974), but an accurate count cannot be obtained. The formation of domes by stretch is reversible. When pairs of muscles were stretched and one muscle allowed to shorten back to its resting sarcomere length before fixation, the stretched muscle was covered with domes but the short muscle had a normal surface membrane with neck structures. This suggests that the membrane is not damaged by the formation of domes.

The surface area of the caveolae

The distribution of caveolae in frog muscle is similar to that described in guinea-pig by Rayns et al. (1968). There are two circumferential bands of caveolae located on either side of the Z-line and these are crossed by single longitudinal bands running at a distance variable between 0·5 and

$2\cdot0\,\mu$m, probably marking the location of the interfibrillar spaces. At low magnification (Pl. 2) the caveolae give the membrane a checkerboard appearance.

The surface area of the caveolae, C, had to be estimated from thin sections (Pl. 3A). The outline tends to be slightly elliptical, with a long diameter parallel to the surface of $81\cdot6\pm11\cdot7$ nm (mean of fifty-eight observations ±1 S.E. of mean) and a shorter diameter perpendicular to the surface of $66\cdot9\pm7\cdot9$ nm. The calculated area of a regular ellipse with these average dimensions is $1\cdot83\times10^{-2}\,\mu$m^2.

Caveolae are often multiple, i.e. two or more caveolae join one another and have a common opening to the extracellular space (Zampighi *et al.* 1974). The number of caveolae connected to the surface by each neck was estimated by comparing the separation between necks, as seen with freeze-fracture, with the centre to centre distance between caveolae as seen in longitudinal sections at the edges of fibres (see for example, Pl. 3 A). To make the two figures consistent, parallel lines were drawn on the exposed fracture faces of the plasmalemma with longitudinal orientation, and at distances equivalent to one-and-a-half-times the thickness of a thin section, i.e. approximately 150 nm. The position of each neck, within the parallel lines, was projected on to one of the lines and the separation between the projected points of the necks measured. The average distance between points was $0\cdot34\pm0\cdot4\,\mu$m (mean ±1 S.E. of mean of 649 measurements), whereas the separation between caveolae in longitudinal sections was $0\cdot17\pm0\cdot04\,\mu$m (mean ±1 S.E. of mean of 484 measurements). The ratio is two, indicating that there are twice as many caveolae as openings.

An independent estimate of caveolar multiplicity was obtained by counting the number of caveolae in glycerol-treated fibres where all are in the dome configuration (Dulhunty & Gage, 1973; Dulhunty & Franzini-Armstrong, 1974). In normal sartorius fibres, at a sarcomere length of $2\cdot2\,\mu$m, the number of necks per square micrometer was twenty-two, while the number of domes in a glycerol-treated sartorius fibre, at the same sarcomere length was fifty. Once again the ratio is approximately two.

The relative areas of caveolae and plasmalemma can be calculated with greatest accuracy in fibres at the critical sarcomere length where there are no folds. In the sartorius muscle this is about $2\cdot8\,\mu$m and there are approximately $18\cdot5$ necks/μm^2 at this sarcomere length (see Text-fig. 4). This indicates a total of 37 caveolae/μm^2 with a combined fractional area, β, of $0\cdot68$ for each square micrometer of the apparent surface area.

Variations with stretch

Three different methods were used to obtain quantitative data from freeze-fracture replicas of muscles fixed at different sarcomere lengths. The methods were: (1) measurement of the relative distribution of caveolae in the neck and dome states; (2) counting the number of caveolar necks covering a constant plasmalemmal area at each sarcomere length; (3) counting the number of caveolar necks covering one square micrometer of apparent surface area. The first two methods were used to obtain information on the way in which the caveolae open to provide membrane necessary for stretch. The third method gave a measure of plasmalemma folding.

Two assumptions were made in the analysis of the data: maintained constant volume, which has been verified (Blinks, J. R., personal communication) for sarcomere lengths shorter than 3·0 μm, and circular cross-section.

Diameter and distribution of necks

In the histograms of Text-fig. 2, the diameter of the caveolar necks (cross-hatched area) and of the domes resulting from their opening (stippled areas) have been plotted as a function of their relative frequency for sartorius (*a* to *d*) and semitendinosus (*e* to *h*). Each histogram is from a different muscle and the average sarcomere length of the fibres is indicated. The total number of necks measured is given in each histogram. The analysis has two advantages. First, since the caveolae are multiple, the effect of their opening is amplified. Thus even a few caveolae in the dome configuration are detected and indication of the sarcomere length at which the caveolae begin to open can be obtained. Secondly, the data in the histograms is independent of the variability in the total number of caveolae on the fibre surface, and of folding of the plasmalemma. Data from sartorius and semitendinosus muscles can be compared by this method. On the other hand, a shortcoming of this particular analysis is that those caveolae which have completely flattened on to the plane of the membrane are not recorded. Thus at long sarcomere lengths, where the number of flattened caveolae becomes significant, the histograms do not accurately reflect the number of domes.

At all sarcomere lengths there is a population of neck diameters distributed around a mean of 34·3 nm. The frequency curve is skewed to the left indicating a minimum size for the necks. A small percentage of the necks have a larger diameter and their size partially overlaps with that of the domes. At short sarcomere lengths (below 2·4 μm, Text-fig. 2*a*, *b*, *c*) the majority of the caveolae are still in the neck configuration with less than 2·6% present as domes. At a longer sarcomere length, 2·8 μm
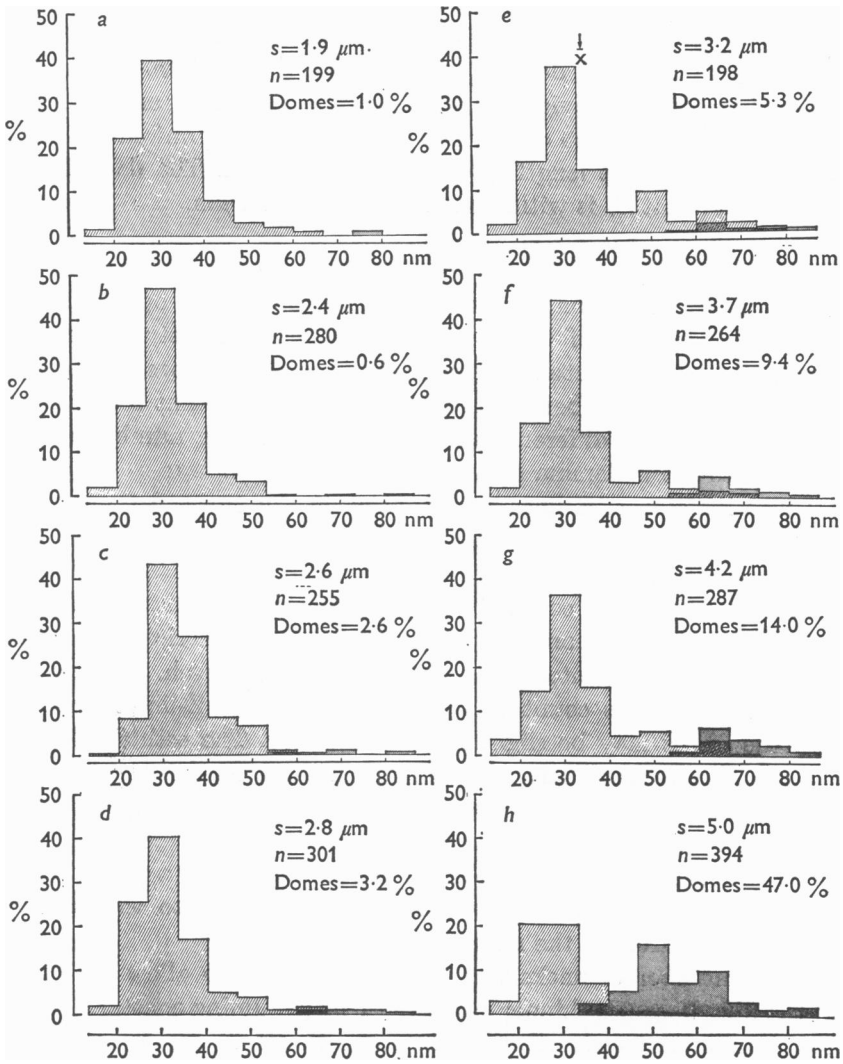
Text-fig. 2. The relative frequency histograms of caveolar neck diameters (cross-hatched areas) and dome diameters (stippled areas), in nm, from muscle fibres at various sarcomere lengths. Fibres were from the sartorius muscle (*a*, *b*, *c*, and *d*) and the semitendinosus muscle (*e*, *f*, *g*, and *h*). The sarcomere length, *s*, number of observations, *n*, and the relative number of domes are indicated on each histogram.

(Text-fig. 2*d*) more than 3 % of the caveolae appear as domes (indicating the opening of 1·5 % of the caveolae) and at 3·2 μm (Text-fig. 2*e*) there are 5·3 % appearing in the dome configuration. At very long lengths (5·0 μm) there are 47 % domes (Text-fig. 2*h*). At these longer sarcomere lengths there is little evidence of membrane wrinkling or folding suggesting that the caveolae open when the membrane is unfolded and that the critical sarcomere length (S_c) has been reached. The data in Text-fig. 2 indicate that S_c is within the range of 2·8–3·2 μm.

The number of necks on the fibre surface

The aim of this section is to see whether the caveolae open to provide a significant amount of the membrane necessary for stretch in either the normal range of stretch or in excessively stretched fibres. This is done by comparing the number of necks occupying a constant reference area of plasmalemma at different sarcomere lengths. The number of necks per reference plasmalemma area was obtained as follows:

(1) The location of Z-lines was marked on the exposed fracture faces and a total count made of necks over an area including the length of one to two sarcomeres and extending for 5–8 μm in a circumferential direction. Two to four fibres were counted for each point, except for semitendinosus fibres at very long sarcomere lengths (see Methods section), where individual fibres were counted for each point on the graph. The source of greatest error in this count was the location of the Z-line, particularly where the fibrils may be slightly out of register. The estimated error is $\pm$ 0·1 μm. The average sarcomere length in the area measured was used as a reference and it was assumed that the section of fibre where counts were made had a uniform sarcomere length.

(2) The necks were referred to an apparent area having a circumferential dimension 1 μm and a longitudinal dimension equal to the sarcomere length, as measured on the micrograph.

(3) The number of necks was further corrected to allow for the fact that the fibre becomes thinner as it lengthens (assuming constant volume). From eqn. 3, the circumference is proportional to $1/\sqrt{S}$. Thus, if the circumferential dimension of the area of measurement is 1 μm when the sarcomere length is 1·9 μm, it will be $[1 . \sqrt{(1\cdot9/S)}] \mu$m at sarcomere length S.

The final area of measurement at a sarcomere length of S is

$$\left[S \ \mu\text{m}. \ 1 \ \mu\text{m}. \ \sqrt{\frac{1\cdot9 \ \mu\text{m}}{S \ \mu\text{m}}} \right] = \left[S \sqrt{\frac{1\cdot9}{S}} \right] \mu\text{m}^2.$$

Thus the number of necks counted over an area with a longitudinal dimension of S and a circumferential dimension 1 μm was corrected to the reference area by multiplying by $\sqrt{(1\cdot9/S)}$.

After the above correction for constant volume the number of necks per reference plasmalemmal area should not vary with folding unless the number of necks over the entire fibre surface changes. A reduction in the corrected number of necks is thus indicative of caveolae opening into the dome configuration.
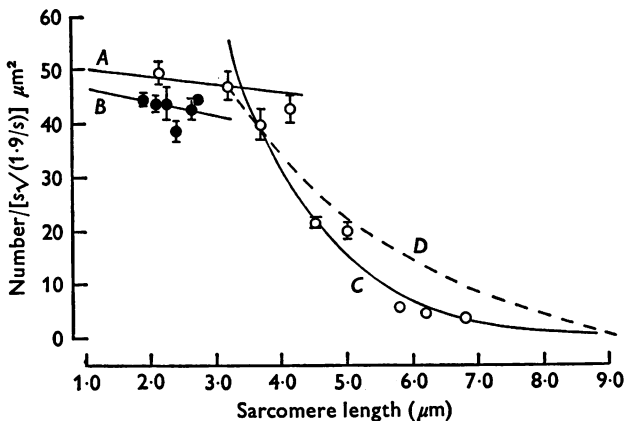
Text-fig. 3. The number of caveolar necks, N^*, measured over a constant plasmalemma area, $[s\sqrt{(1\cdot9/s)}]\ \mu m^2$ (ordinate) is plotted against sarcomere length (abscissa). Filled circles show results from sartorius fibres and open circles show results from semitendinosus fibres. The vertical bars indicate ± 1 S.E. of mean. Line A is a linear regression through the results from individual semitendinosus fibres at sarcomere lengths less than $3\cdot2\ \mu m$. Line B is a linear regression line through the results from individual sartorius fibres. Line C is an exponential regression line through the results from individual semitendinosus fibres at sarcomere lengths greater than $3\cdot2\ \mu m$. See text for details on the significance of lines A, B, and C. Line D has been predicted from the constant volume equations with the assumption that β is equal to $2Nc$ at sarcomere lengths greater than $3\cdot2\ \mu m$. The text should be consulted for details of the derivation of curve D.

Text-fig. 3 shows the corrected average number of necks per reference plasmalemmal area in fibres from the sartorius (filled circles) and the semitendinosus (open circles). The vertical bars denote one standard error of mean. The average values have been subdivided into three groups and regression analyses done on the individual data from points occurring within each group. The groups are: (i) data from sartorius muscles which were always at sarcomere lengths less than $2\cdot8\ \mu m$; (ii) data from semitendinosus fibres with sarcomere lengths $3\cdot2\ \mu m$ and less and (iii) data from semitendinosus fibres with sarcomere lengths greater than $3\cdot2\ \mu m$.

For groups (i) and (ii) above the points were fitted by linear regression

lines, A and B, respectively; line A has a slope of -2.5 and a correlation coefficient of 0.02 and line B has a slope of -1.7 and a correlation coefficient of 0.02. There is however no significant difference between the numbers of necks at 2.0 or at $3.2\ \mu$m for either group (Student's t test, $0.3 < P < 0.5$). Thus we can conclude that there is no significant change in the number of caveolae occupying the reference plasmalemmal area at sarcomere lengths less than $3.2\ \mu$m.

The average values for the sartorius muscle in this range of sarcomere lengths were slightly less than those for the semitendinosus muscle. This tendency was consistently found but the difference was not statistically significant.

The data falling into group (iii), as defined above, show a progressive decrease with increasing sarcomere length: e.g. points at a sarcomere length $4.5\ \mu$m are significantly lower than those at $3.6\ \mu$m (Student's t test, $P < 0.001$). The points were fitted by an exponential regression line (curve C, Text-fig. 3) with a correlation coefficient 0.88. This curve should indicate the length to which the fibres must be stretched in order to open all the necks. The sarcomere length at which all the necks are open is S_0. Curve C falls below one neck per reference area at a sarcomere length of $8.6\ \mu$m and so S_0 is $8.6\ \mu$m from this curve.

S_0 can be calculated independently using assumptions of constant volume and constant total plasmalemma.

For the particular case of sarcomere lengths, S_2, greater than S_c, $\alpha = 0$ (see Table 3), the total plasmalemma per unit area, M_2, is defined as:

$$M_2 = \frac{TP_2}{A_2} = 1 + \beta_2.$$

At S_0,
$$\beta_0 = 0 \quad \text{and} \quad M_0 = 1.$$

The ratio of M_c and M_0 is

$$\frac{M_c}{M_0} = \frac{TP_c}{TP_0} \cdot \frac{A_0}{A_c}. \tag{17}$$

TP is a constant and thus, if constant volume and constant plasmalemma area are maintained, eqn. 6 can be combined with eqn. 17 and

$$\frac{M_c}{M_0} = \sqrt{\frac{S_0}{S_c}}. \tag{18}$$

By definition, $M_0 = 1$ and thus

$$M_c = \sqrt{\frac{S_0}{S_c}}, \tag{19}$$

and
$$S_0 = (M_c)^2 \cdot S_c. \tag{20}$$

For the semitendinosus muscle S_c has a value of $3.2\ \mu$m and M_c is 1.7 (see Table 5). Thus the numerical solution of eqn. 17 is

$$S_0 = 3.2\ (1.7)^2 = 9.1\ \mu\text{m}.$$

This independently calculated value of S_0 is close to that obtained from the regression line through the points of measured values.

It is interesting to compare the way in which the necks open with stretch (curve C, Text-fig. 3) with the curve that can be predicted for the necks opening, one at a time, to provide the membrane necessary for stretch (curve D, Text-fig. 3).

Curve D has been constructed using the assumptions of constant volume and constant plasmalemma. It is necessary to derive a relationship between the normalized number of necks, N, the caveolar plasmalemma area, β, and sarcomere length for $S_2 > S_c$. From Table 3 it can be seen that for $S_2 > S_c$, $n_x = n_c(1-\gamma)$. Thus eqn. 7 can be rewritten for $S_2 > S_c$ in the following way:

$$\frac{N_2}{N_c} = \frac{n_c(1-\gamma)}{n_c} \cdot \frac{A_c}{A_2} = (1-\gamma)\frac{A_c}{A_2}. \tag{21}$$

If we assume that the necks open, one at a time, to provide membrane and therefore that γ is proportional to $\sqrt{S}$, N_2 can be related to S_2 by the constant volume eqn. 6.

$$\frac{N_2}{N_c} = (1-\gamma)\sqrt{\frac{S_c}{S_2}}. \tag{22}$$

Similarly for β, when $S_2 > S_c$, $\beta = (J/A)$ and $J_c = 2nc$ and $J_2 = 2n(1-\gamma)c$. Eqn. 10 can be written for $S_2 > S_c$ (again using the assumption that γ is proportional to $\sqrt{S}$).

$$\frac{\beta_2}{\beta_c} = \frac{2c(1-\gamma)n}{2cn}\sqrt{\frac{S_c}{S_2}} = (1-\gamma)\sqrt{\frac{S_c}{S_2}}. \tag{23}$$

Combining eqns. 22 and 23,

$$\frac{N_2}{N_c} = \frac{\beta_2}{\beta_c}. \tag{24}$$

The relationship between β_2 and S_0 is obtained from eqn. 19, which can be rewritten for $S_2 > S_c$.

$$M_2 = \sqrt{\frac{S_0}{S_2}}. \tag{25}$$

When $S_2 > S_c$, $M_2 = 1 + \beta_2$ (see Table 3), and thus

$$\beta_2 = \sqrt{(S_0/S_2)} - 1. \tag{26}$$

Eqn. 26 can then be combined with eqn. 24:

$$N_2 = (N_c/\beta_c)\,(\sqrt{(S_0/S_2)} - 1). \tag{27}$$

Values assumed for constants used to construct curve C are: $N_c = 47$ necks per reference area; $\beta_c = 0.69$ and $S_0 = 8.9\ \mu m$.

Although the experimental and theoretical curves give similar values for S_0, the number of necks initially opening (curve C) is greater than that predicted by the unfolding curve (curve D). Thus eqn. 27 does not describe the opening of caveolae. The discrepancy between the two curves is due to the fact that the experimental analysis gives information about the transition from necks to domes, but not on the way in which the domes flatten. If the majority of necks open into domes shortly

after S_c and then the domes flatten, in parallel, with further stretch the loss of the necks (i.e. increase in γ) with stretch should be exponential and thus deviate from the predicted binomial curve. Thus N cannot be simply related to β with the constant volume equations when the caveolae are opening.

Number of necks per square micrometer and plasma membrane folding

Membrane folding is visible on the exposed fracture faces of fibres fixed at short sarcomere lengths (Pl. 1). However, since freeze-fracture gives only an image of the apparent membrane area, it is not possible to measure membrane folding directly by this technique. A measure of membrane folding must be obtained indirectly by counting the number of necks on a unit area of the apparent surface membrane.
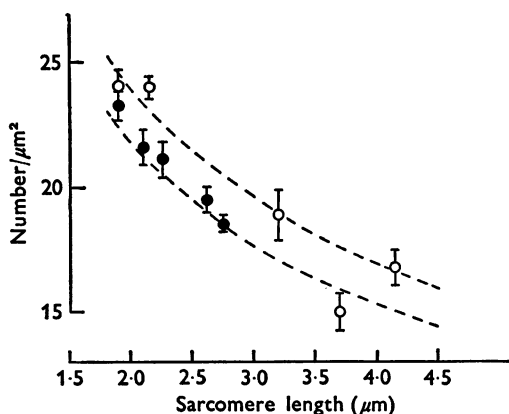
Text-fig. 4. The average number of caveolar necks, N, per square micron of apparent surface area (ordinate) plotted as a function of sarcomere length (abscissa). Open circles, semitendinosus muscle fibre; filled circles, sartorius muscle fibre. The vertical bars show ± 1 S.E. of mean. The broken lines show curves predicted from the constant volume equations as described in the text.

The number of necks on areas of no less than $10\ \mu m^2$ were counted on each of five micrographs of fibres at each sarcomere length and the results are shown in Text-fig. 4. Filled circles are from sartorius muscles and open circles from semitendinosus muscles. The vertical bars represent ± 1 S.E. of mean. The analysis was not done at sarcomere lengths greater than S_c because folding does not contribute to membrane area at longer sarcomere lengths. The data shown in Text-fig. 4 can be used to estimate membrane folding because we have shown that the total number of caveolae remain constant at sarcomere lengths less than $2 \cdot 8$–$3 \cdot 2\ \mu m$

(Text-fig. 3, lines A and B) and so apparent variations in the number of caveolae per square micrometer which accompany changes in sarcomere length below S_c (Text-fig. 4) should provide a direct measure of membrane folding.

The two curves (dashed lines) in Text-fig. 4 illustrate the theoretical variation in the number of necks per square micrometer of apparent surface for two fibres having an S_c 3·2 μm and a density (measured, semitendinosus) of necks 18·9/μm^2 (upper curve) and an S_c 2·8 μm and density (measured, sartorius) of necks 18·5/μm^2 (lower curve).

The theoretical curves were calculated from eqn. 9. Since the total number of caveolae do not change when $S < S_c$ (see Text-fig. 3) the apparent change in the number of caveolae per unit area should be directly proportional to membrane folding, i.e.

$$N_1 = N_c \sqrt{\frac{S_c}{S_1}},$$

where N_1 is the number of necks (per unit of apparent surface area) at sarcomere length S_1 and N_c is the number of necks at the critical sarcomere length. S_1 is any sarcomere length less than S_c.

In Text-fig. 4 all the measurements fall within the area delimited by the two calculated curves and the line of best fit through the measured points would describe a similar curve. If S_c were taken at some value longer than 3·2 μm, and the observed number of necks (Text-fig. 4) for that length used in eqn. 9, the theoretical curve would be lower than the measured points because of the true reduction in the number of necks as the sarcomere length increases beyond S_c. This emphasizes the point that eqn. 8 is true only for sarcomere lengths less than S_c.

From the agreement between the experimental data and the theoretical curves we conclude: (i) the assumption that there is folding of the membrane below a critical sarcomere length is correct; (ii) in agreement with the data presented in the two previous sections, the absolute number of caveolae at sarcomere lengths less than S_c does not change and (iii) the critical sarcomere length is somewhere between 2·8 and 3·2 μm in the sartorius and semitendinosus muscles.

DISCUSSION

The main aim of this paper was to find out how much plasmalemma is contained in membrane folds and caveolae and to express these as fractions of the apparent surface area (A). The results presented above enable a systematic definition of the variation in the fractional areas of the folds (α) and of the caveolae (β) at different sarcomere lengths. The

freeze-fracture replicas used to count the numbers of caveolae are ideal for surveying large areas of membrane, but cannot be used to measure the height of the folds, and thus a quantitative definition of folding has to be obtained indirectly. Eqns. 11 and 16 (see Methods section) give simple equations for determining β and α and the derivation of these is dependent on three assumptions which have been tested in the results section. The first two assumptions, used in determination of α, are that the volume and total plasmalemma area of the fibre are constant. The third assumption, used in the determination of β, is that the total number of caveolae is constant for $S < S_c$ and that any variation in the number of necks per square micrometer of apparent surface is due to folding (verified in Text-fig. 3). Text-fig. 4 shows that variation in the number of necks per square micrometer of apparent surface can be described by eqn. 9, which incorporates all three assumptions. Values of α and β have been calculated, using eqns. 11 and 16 respectively, and the results for the sartorius are given in Table 4 and for the semi-tendinosus in Table 5.

TABLE 4. Plasmalemmal area of sartorius fibres at different sarcomere lengths

Sarcomere length (μm)	α	β	Total area $A + \alpha A + \beta A$
1·8	0·24	0·84	2·08A
2·0	0·18	0·80	1·98A
2·2	0·13	0·77	1·90A
2·4	0·08	0·73	1·81A
2·6	0·04	0·71	1·75A
2·8	0·00	0·68	1·68A

TABLE 5. Plasmalemmal area of semitendinosus fibres at different sarcomere lengths

Sarcomere length (μm)	α	β	Total area $A + \alpha A + \beta A$
1·8	0·33	0·92	2·24A
2·0	0·26	0·87	2·13A
2·2	0·20	0·83	2·03A
2·4	0·15	0·79	1·93A
2·6	0·10	0·76	1·86A
2·8	0·07	0·74	1·81A
3·0	0·03	0·71	1·74A
3·2	0·00	0·69	1·69A

β_c was calculated from the number of necks per square micrometer (Text-fig. 4) at the critical sarcomere length. It was assumed that there are twice as many caveolae as necks (see Results section) and that the

average caveolar area is $1.83 \times 10^{-2} \mu m^2$ (see Results also). In the calculation of α and β for the sartorius (Table 4), S_c was taken as $2.8 \mu m$ and β_c as 0.68. In the same calculations for the semitendinosus (Table 5), S_c was taken as $3.2 \mu m$ and the value of β_c as 0.7. The critical sarcomere length of the sartorius muscle is shorter than that of the semitendinosus. Fractured membranes of sartorius fibres with sarcomere lengths of $2.8 \mu m$ appeared to be unwrinkled, but the fibres could not be stretched further and so it was not possible to determine the critical sarcomere length more accurately. It is possible that the values of plasmalemma area estimated for the sartorius muscle (Table 4) are less than the true values because of an artificially low critical sarcomere length. For example, if S_c were 3.2 instead of $2.8 \mu m$, the total plasmalemma area, at a sarcomere length $2.4 \mu m$, would be $1.93A$ instead of $1.81A$.

Most physiological experiments are done with muscles held at sarcomere lengths 2.4–$2.8 \mu m$. The total plasmalemmal area for the sartorius muscle, at these sarcomere lengths, is $1.84A$ to $1.67A$ (Table 4). The results given so far have not been corrected for shrinkage during preparation for freeze-fracture. There is a maximum of 4% circumferential shrinkage during glycerol infiltration (see Tables 1, 2). When this is taken into account in calculations of the fractional contribution of the caveolae to the sartorius plasmalemma, β_c is reduced to 0.64 and the plasmalemma area, at a sarcomere length $2.4 \mu m$, is $1.80A$.

It is interesting to speculate on the way in which the increased plasmalemma area, following consideration of folds and caveolae, will alter the specific electrical properties previously assigned to the surface membrane of skeletal muscle. For brevity the discussion will be confined to the sartorius muscle. The area increment from membrane folding is numerically smaller than that from the caveolae and its effect on the electrical properties can be stated simply. Folding increases the plasmalemma area by 10% at a sarcomere length of $2.4 \mu m$ (Table 4) and thus estimates of membrane resistance would be 10% too low and estimates of membrane capacitance 10% too high. Studies on the effects of length changes on action potential conduction velocity confirm the idea that membrane folding does not cause any more complex changes of the electrical properties of the surface membrane (Hodgkin, 1954; Martin, 1954). The caveolae present a more complex problem. Their contribution to the electrical parameters of the fibre will depend on the electrical continuity between the caveolar lumen and the external solution and also on the resting conductance of the caveolar membrane. In contrast to the lumen of the elongated tubular system, the lumen of the spherical caveolae should not present a significant series resistance. The caveolar neck, however, may provide an access resistance to the caveolae. So far this has not been experimentally determined. Easy access to extracellular markers, of large molecular weight, is often used as evidence for continuity of the T-tubules and can likewise be used as circumstantial evidence for continuity of the caveolae. A theoretical convergence resistance can be calculated for the neck of the caveolae; however this is small and would not be expected to electrically isolate the caveolar membrane. The fact that the caveolar membrane has few particles suggests that it may have a high specific

resistance and thus that the measured membrane resistance is essentially the true specific resistance of the non-caveolar membrane, and independent of an access resistance at the mouth of the caveolae.

The specific capacitance of the surface membrane has been determined from square pulse analysis of normal and glycerol treated fibres and impedance analysis of normal and glycerol treated fibres and values calculated from 1·0 to 2·6 $\mu F/cm^2$ (Falk & Fatt, 1964; Gage & Eisenberg, 1969; Schneider, 1970; Hodgkin & Nakajima, 1972; Dulhunty & Gage, 1973; Nakajima & Bastian, 1974; Valdiosera, Clausen & Eisenberg, 1974). Since the caveolae open out and appear as dome structures after glycerol treatment, only the interpretation of the impedance measurement of normal muscle will be affected by the presence of an access resistance at the mouth of the caveolae. Assuming electrical continuity, previous estimates of the specific membrane capacitance must be over-estimates of at least 70 % (for a sarcomere length of 2·4 μm) and this becomes 80 % when folding is considered. The true specific membrane capacitance must be between 0·51 and 1·44 $\mu F/cm^2$. These values can be compared to the calculated capacitance of 0·53 $\mu F/cm^2$ for a lipid bilayer, 5 nm thick and with a di-electric constant of 3·0.

That the fibre maintains constant volume during length changes has often been assumed, but there is little direct evidence. X-ray data (Huxley, 1953; Elliott, 1964) shows that the volume occupied by the myofilaments does not change during shortening, implying that the fibre volume remains constant. Cross-sectional areas measured from optical sections of single fibres, stretched up to a sarcomere length of 3·0 μm show changes that are consistent with the assumption of constant volume (Blinks, J. R., personal communication). In this paper we have used constant volume equations to predict a curve for membrane folding (see eqn. 9) and also to predict the point at which the membrane should rupture (see eqn. 20) with increases in passive stretch. These predictions cover a range of sarcomere lengths from 1·8 to 9·0 μm and there is good correlation with measured values over the entire range. The conclusion from this is that constant volume is maintained at all times, even during excessive and unphysiological stretch. The results are similarly consistent with the idea that the total membrane area is invariant, although the way in which it is arranged around the sarcoplasm alters in a predicted way with stretch. The fibres rupture when all the caveolae are open and there is no further membrane available to increase the surface area. Since the plasmalemma, itself, does not appear to stretch and does not appear to be able to stand significant stretch, once the caveolae have flattened, it seems reasonable to conclude that it is inelastic.

The contribution of the sarcolemma (i.e. plasma membrane, basement membrane and collagen fibrils) to resting tension of muscle fibres has been evaluated in several different ways (Casella, 1950; Podolsky, 1964; Rappoport, 1972). The general conclusion of these investigations is that the sarcolemma has a negligible effect on the resting tension at sarcomere lengths less than 3·0 μm, but becomes increasingly significant with stretch

beyond this sarcomere length. Rappoport (1972) has suggested that the tension exerted by the sarcolemma, at long sarcomere lengths, is due to the basement membrane and outer connective tissue components; he considers the contribution of the plasmalemma itself to be insignificant. Our results show that unfolding of plasmalemma folds provides sufficient membrane area for stretch up to approximately $3 \cdot 0\ \mu$m. It is possible that basement membrane and plasmalemma layers fold in parallel in this physiological range of stretch. In the same range of sarcomere lengths the collagen fibrils change from a slack, oblique configuration, to an orientation parallel to the fibre's long axis (Schmalbruch, 1974). For further stretch the caveolae can act as 'safety valves' to prevent damage to the plasmalemma, but the basement membrane and connective tissue layers must be rearranged to accommodate the increase in length. As mentioned previously, the plasmalemma (seen in freeze-fracture replicas) ruptures when all the caveolae have opened and flattened. The fibres, viewed macroscopically, break when stretched to a similar sarcomere length. If all the tension is exerted by the non-plasmalemmal components of the membrane then their elastic limit must be reached when all the caveolae have flattened otherwise the connective tissue could continue to stretch after plasmalemma rupture and the muscles would appear to be intact. The alternative is that the tension is exerted by the plasmalemma and that the increase seen at sarcomere lengths greater than $3 \cdot 0\ \mu$m is proportional to the resistance to caveolar opening.

It is interesting that the semitendinosus muscle can be stretched to sarcomere lengths that are almost three times greater than the maximum sarcomere length possible in the sartorius muscle. The results presented in Text-figs. 3 and 4 show that the numbers of caveolae in the two muscles are approximately equal and presumably the potential ability of the plasmalemma to accommodate stretch is the same. We have observed that single fibres from the sartorius can be stretched to longer sarcomere lengths than the whole muscle, while single semitendinosus fibres cannot be stretched to lengths as great as those of fibres in the whole muscle. These observations suggest that the difference in the ability of the two muscles to survive stretch is partly related to the arrangement of the connective tissue holding the fibres together and may be wholly related to the elasticity of the basement membrane and connective tissue. A possible alternative is that resistance to caveolar opening is greater in the sartorius muscle. This seems unlikely because the ability of the caveolae to open is presumably a complex function of their surface tensions and of the lipid and protein of their membranes. It is unlikely that these intrinsic properties would differ significantly between the two muscles.

The physiological role of the caveolae is still obscure. It seemed reasonable that they may act as a reservoir of membrane for stretch. However our results show that they do not function in this way in the physiological range of stretch. Their ability to provide membrane for stretch to sarcomere lengths greater than $3 \cdot 2 \mu m$ is probably more fortuitous than functional. The caveolae are probably not actively pinocytotic. They readily fill with extracellular markers which are not redistributed in the cytoplasm. There are three other facts which together deny a pinocytotic role. The basement membrane can often be seen to follow the plasmalemma invagination into the caveolae and is particularly obvious in preparations stained with ruthenium red (Dulhunty & Gage, 1973). The caveolar outlines remain clear after dome formation in glycerol-treated and hypotonic-treated muscles (Dulhunty & Franzini-Armstrong, 1974). Finally, the domes formed after excessive stretch are capable of reforming the normal neck structure when the muscles are released from stretch. These observations all suggest that the caveolae are specialized structural components of the surface membrane.

It is possible that the caveolae are an integral part of the T-system (Zampighi *et al.* 1974) since T-tubules develop from caveolar like structures in embryonic muscle (Ezerman & Ishikawa, 1967; Schiaffino & Margreth, 1968). The T-system can often be seen to open into the caveolae as well as on to the surface membrane (Rayns *et al.* 1968; C. Franzini-Armstrong, L. Landmesser & G. Pilar, to be published; Zampighi *et al.* 1974). The presence of all the caveolae in their spherical form does not seem to be required for the normal function of the T-tubules in excitation–contraction coupling. When sartorius or semitendinosus fibres are exposed to Ringer with an osmotic strength 0·5 that of normal Ringer they swell, following water influx, increasing their volume by approximately 80 % (Franzini-Armstrong, C. & Dulhunty, A., unpublished observations) and at the same time approximately 50 % of the caveolae open and form a dome-structure (Dulhunty & Franzini-Armstrong, 1974). Okada & Gordon (1972) studied membrane potentials, action potentials and twitches in hypotonic solutions. They found that all three parameters were unaffected by exposure to 0·5 Ringer. Thus excitation–contraction coupling is not affected by the opening of 50 % of the caveolae.

Other possible functions for the caveolae are either a metabolic function or they may simply serve to increase the surface-to-volume ratio of the fibres.

REFERENCES

ANDERSSON-CEDERGREN, E. (1959). Ultrastructure of motor end-plate and sarcoplasmic components of mouse skeletal muscle fibre as revealed by three-dimensional reconstructions from serial sections. *J. Ultrastruct. Res.* suppl. 1, 1.

BENNETT, H. S. (1960). In *The Structure and Function of Muscle*, vol. 1, ed. BOURNE, G. H., pp. 137–150. New York: Academic Press.

BLINKS, J. R. (1965). Influence of osmotic strength on cross-section and volume of isolated single muscle fibres. *J. Physiol.* **177**, 42–57.

CASELLA, C. (1950). Tensile force in total striated muscle, isolated fibre and sarcolemma. *Acta physiol. scand.* **21**, 380–401.

DULHUNTY, A. F. & FRANZINI-ARMSTRONG, C. (1974). Caveolae as specialized structural components of the surface membrane of skeletal muscle. *Fedn Proc.* **33**, no. 3, 401 P.

DULHUNTY, A. F. & GAGE, P. W. (1973). Electrical properties of toad sartorius muscle fibres in summer and winter. *J. Physiol.* **230**, 619–641.

EISENBERG, B. (1972). Three dimensional branching of the T-system in frog sartorius muscle. *J. cell Biol.* **55**, 68a.

EISENBERG, R. S. & GAGE, P. W. (1969). Ionic conductances of the surface and transverse tubular membranes of frog sartorius fibres. *J. gen. Physiol.* **53**, 279–297.

ELLIOTT, G. F. (1964). X-ray diffraction studies on striated and smooth muscles. *Proc. R. Soc.* B **160**, 467–472.

EZERMAN, E. B. & ISHIKAWA, H. (1967). Differentiation of the sarcoplasmic reticulum and T-system in developing chick skeletal muscle *in vitro*. *J. cell Biol.* **35**, 405–420.

FALK, G. & FATT, P. (1964). Linear electrical properties of striated muscle fibres observed with intracellular electrodes. *Proc. R. Soc.* B **160**, 69–123.

FRANZINI-ARMSTRONG, C. (1973). Membrane systems in muscle fibres. In *The Structure and Function of Muscle*, vol. 1, ed. BOURNE, G. H., pp. 532–617. New York: Academic Press.

GAGE, P. W. & EISENBERG, R. S. (1969). Capacitance of the surface and transverse tubular membrane of frog sartorius muscle fibres. *J. gen. Physiol.* **53**, 265–277.

HODGKIN, A. L. (1954). A note on conduction velocity. *J. Physiol.* **125**, 221–224.

HODGKIN, A. L. & NAKAJIMA, S. (1972). Analysis of the membrane capacity in frog muscle. *J. Physiol.* **221**, 121–136.

HUXLEY, H. E. (1953). X-ray analysis and the problem of muscle. *Proc. R. Soc.* B **141**, 59–62.

KATZ, B. (1948). The electrical properties of the muscle fibre membrane. *Proc. R. Soc.* B **135**, 506–534.

MARTIN, A. R. (1954). The effect of change in length on conduction velocity. *J. Physiol.* **125**, 215–220.

NAKAJIMA, S. & BASTIAN, J. (1974). Double sucrose gap applied to single muscle fibres of *Xenopus laevis*. *J. gen. Physiol.* **63**, 235–256.

OKADA, R. D. & GORDON, A. M. (1972). Excitation, contraction and excitation–contraction coupling of frog muscles in hypotonic solutions. *Life Sci. Oxford* **11**, pt. 1, 449–460.

PAGE, S. (1964). The organization of the sarcoplasmic reticulum in frog muscle. *J. Physiol.* **175**, 10–11 *P*.

PEACHEY, L. D. (1965). The sarcoplasmic reticulum and transverse tubules of the frog's sartorius. *J. cell Biol.* **25**, 209–231.

PEACHEY, L. D. & SCHILD, R. F. (1968). The distribution of the T-system along the sarcomeres of the frog and toad sartorius muscles. *J. Physiol.* **194**, 249–258.

PEACHEY, L. D. & TERRELL, A. (1974). Surface area of frog muscle fibres at different lengths. In *Proc. Int. Union Physiol. Sci.*, vol. XI, New Delhi, 1974.

PINTO DA SILVA, P. & BRANTON, D. (1970). Membrane splitting in freeze etching. *J. cell Biol.* **45**, 598–605.

PODOLSKY, R. J. (1964). The maximum sarcomere length for contraction of isolated myofibrils. *J. Physiol.* **170**, 110–123.

RAPPOPORT, S. I. (1972). Mechanical properties of the sarcolemma and myoplasm in frog muscle as a function of sarcomere length. *J. gen. Physiol.* **59**, 559–585.

RAYNS, D. G., SIMPSON, F. O. & BERTAUD, W. S. (1968). Surface features of striated muscle. II. Guinea-pig skeletal muscle. *J. cell Sci.* **3**, 475–482.

SCHIAFFINO, S. & MARGRETH, A. (1968). Coordinated development of the sarcoplasmic reticulum and T-system during postnatal differentiation in rat skeletal muscle. *J. cell Biol.* **41**, 855–875.

SCHMALBRUCH, H. (1974). The sarcolemma of skeletal muscle fibres as demonstrated by a replica technique. *Cell Tiss. Res.* **150**, 377–387.

SCHNEIDER, M. (1970). Linear electrical properties of the transverse tubules and surface membrane of skeletal muscle fibres. *J. gen. Physiol.* **56**, 640–671.

TILLACK, T. W. & MARCHESI, V. T. (1970). Demonstration of the outer surface of freeze-etched red blood cells. *J. cell Biol.* **45**, 649–653.

VALDIOSERA, R., CLAUSEN, C. & EISENBERG, R. S. (1974). Impedance of frog skeletal muscle fibres in various solutions. *J. gen. Physiol.* **63**, 460–491.

ZAMPIGHI, E. G., VERGARA, J. & RAMÓN, F. (1975). The connection between the T-tubules and the plasma membrane in frog skeletal muscle. *J. cell Biol.* **64**, 734–740.

EXPLANATION OF PLATES

PLATE 1

The external leaflet (Face *B*) of the plasmalemma of a semitendinosus fibre at a sarcomere length of approximately 2·0 μm. Double arrow, direction of the longitudinal axis of the fibre; dashed lines, approximate positions of the Z-lines. In this and all subsequent micrographs, the single arrow indicates the direction of shadowing. The numerous small circular structures are caveolar necks. These form parallel circumferential bands on either side of the Z-line and also longitudinal bands. The former can be seen more clearly in Pl. 2. Calibration = 1 μm.

PLATE 2

The external leaflet (Face *B*) of the plasma membrane of a sartorius fibre at a sarcomere length of approximately 2·8 μm. This fibre is close to the critical sarcomere length and, in contrast to Pl. 1, the plasmalemma is unfolded. Double arrow, long axis of the fibre; dashed lines, approximate positions of the Z-lines; calibration = 1 μm.
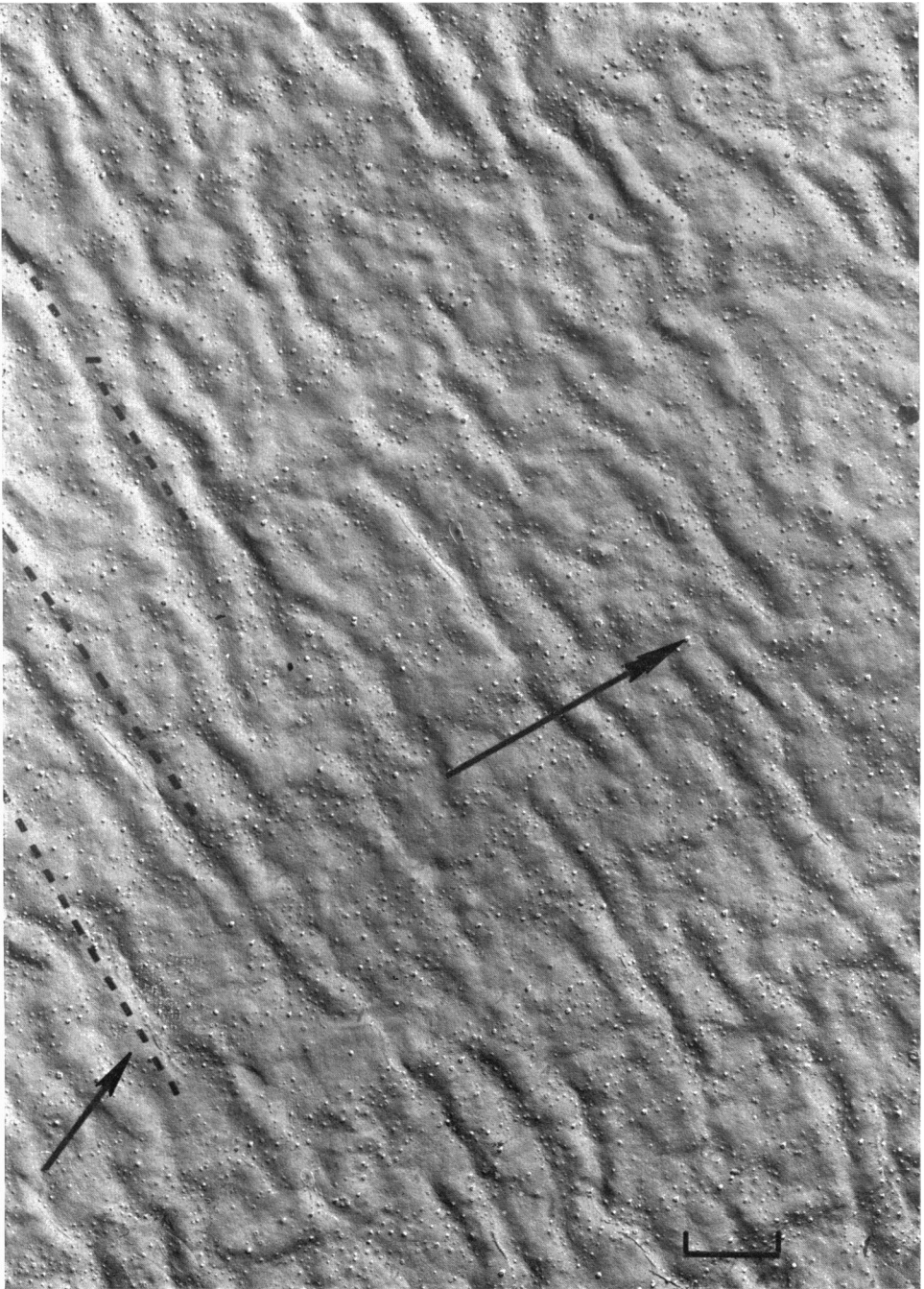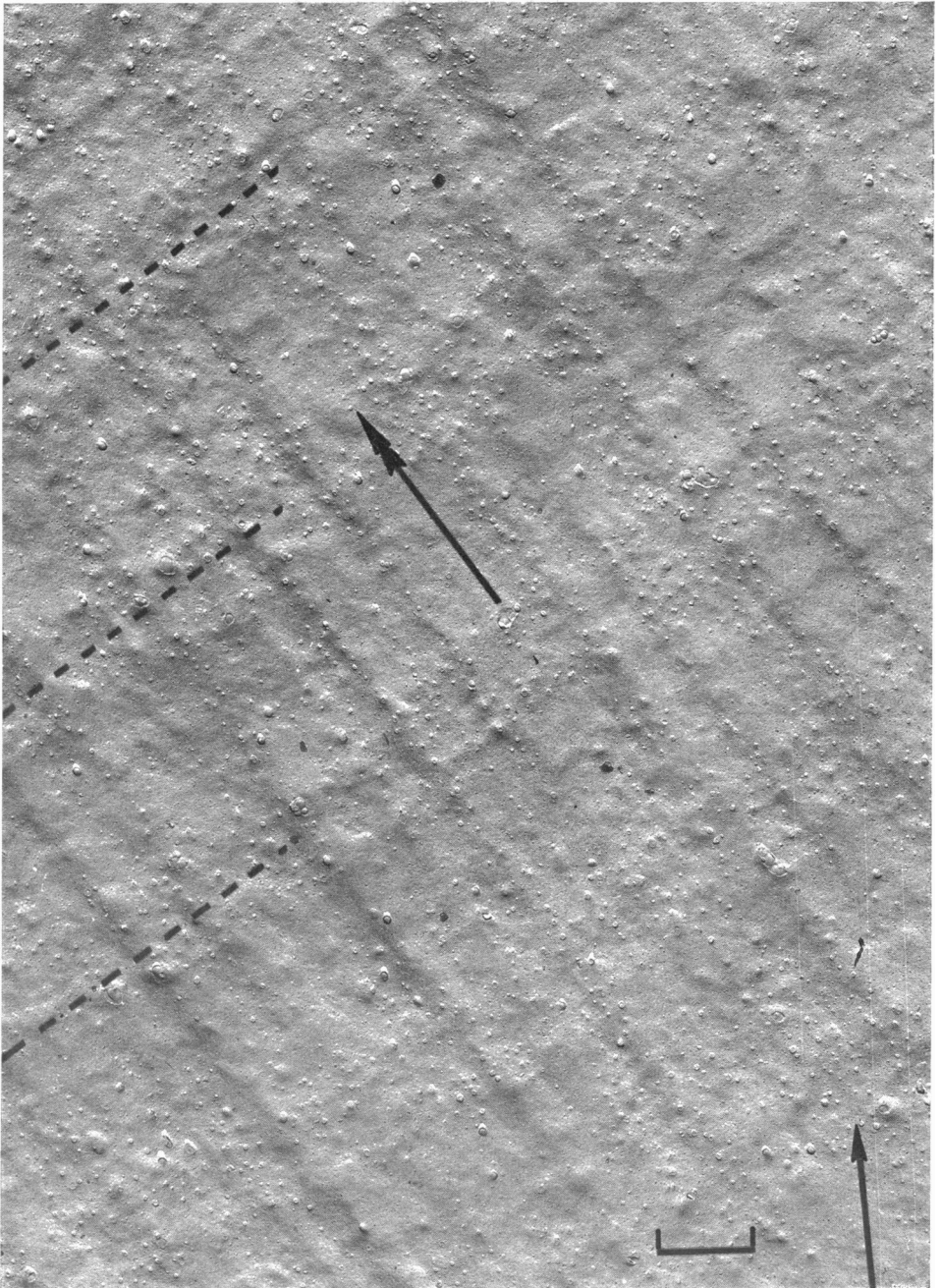
ANGELA F. DULHUNTY AND CLARA FRANZINI-ARMSTRONG   *(Facing p. 538)*
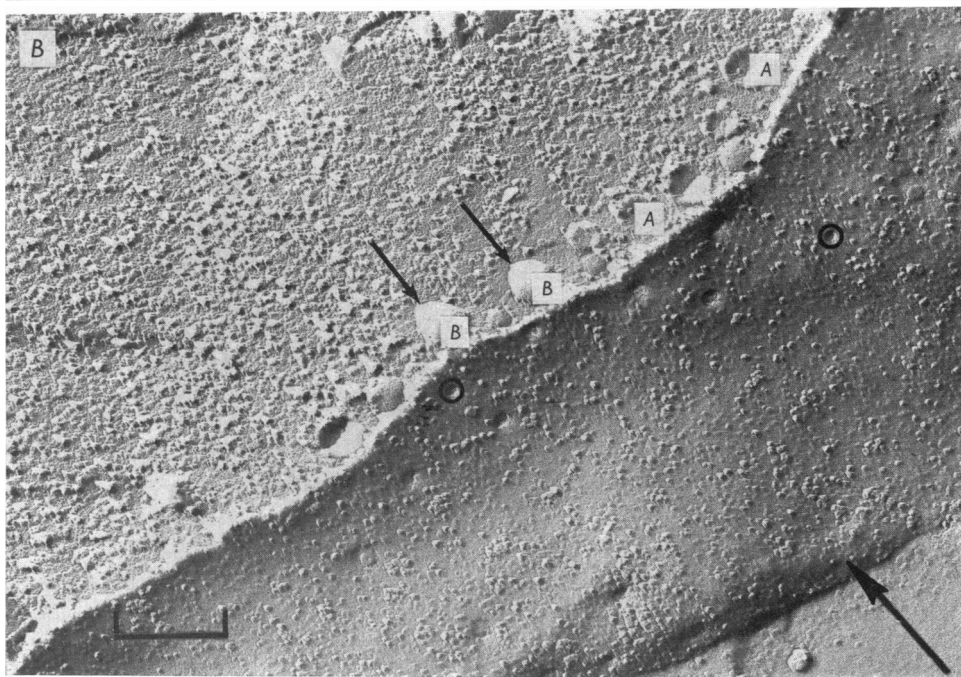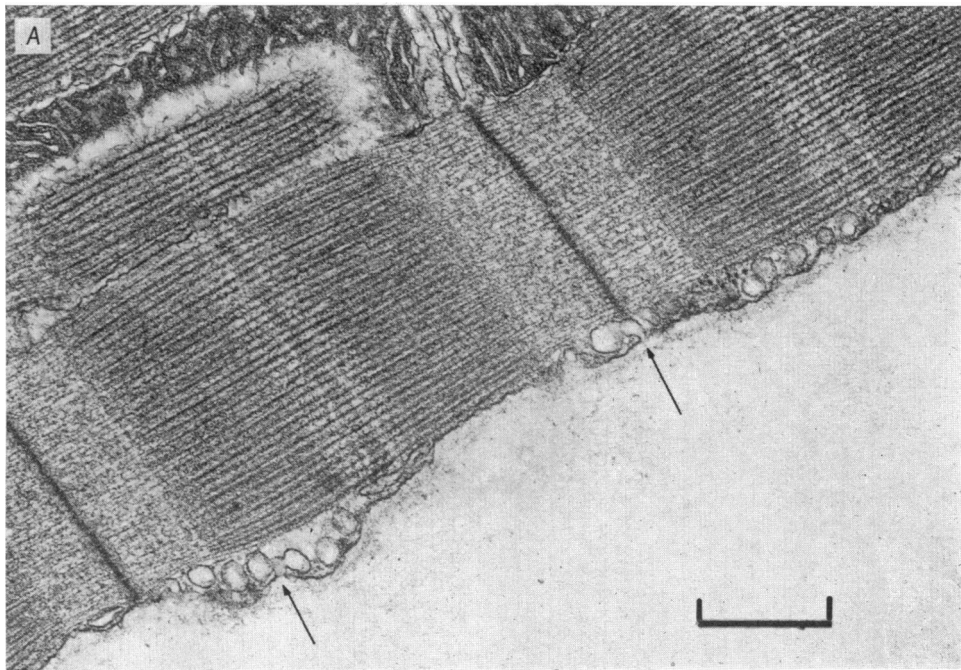
ANGELA F. DULHUNTY AND CLARA FRANZINI-ARMSTRONG

ANGELA F. DULHUNTY AND CLARA FRANZINI-ARMSTRONG
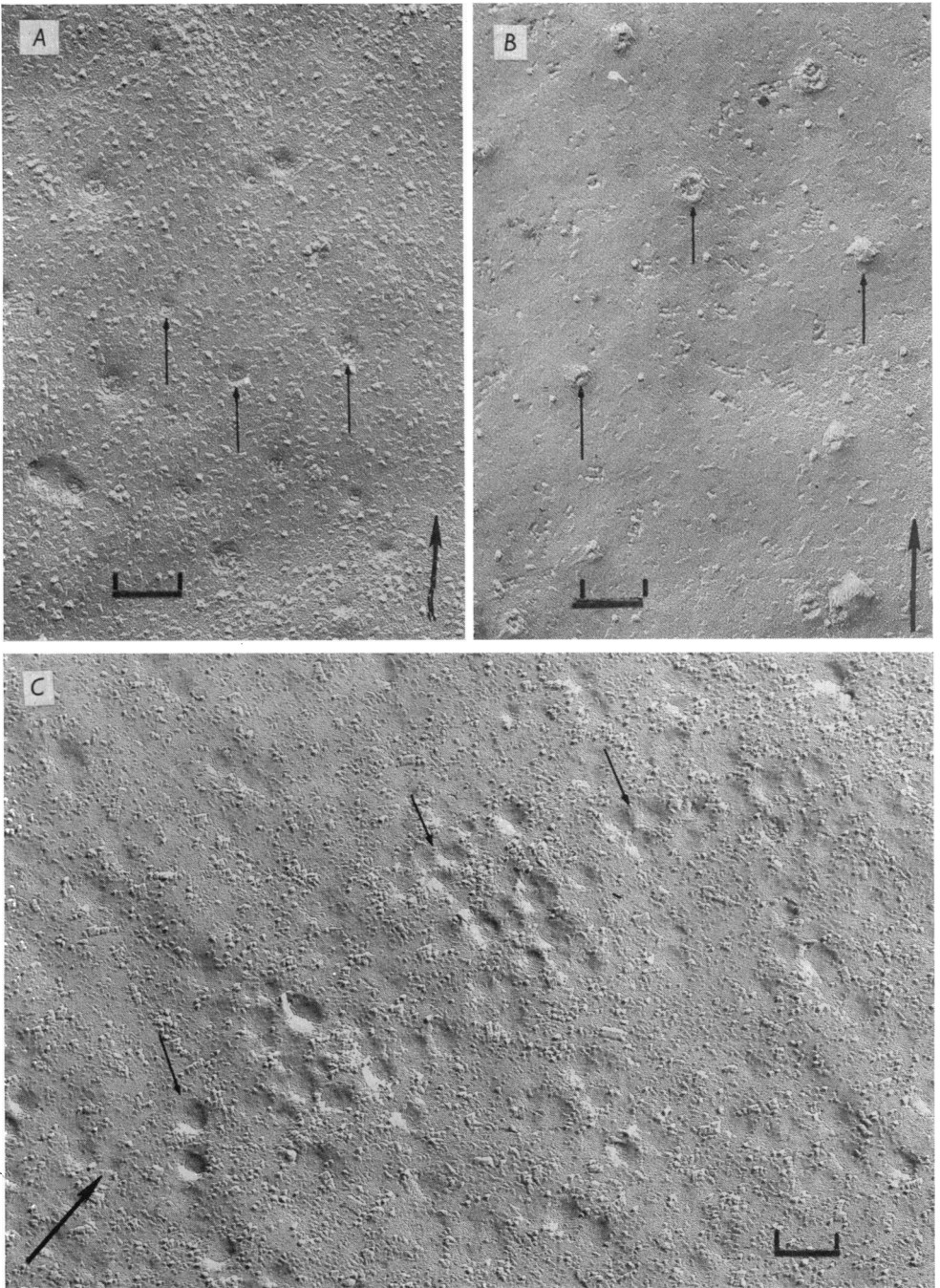
ANGELA F. DULHUNTY AND CLARA FRANZINI-ARMSTRONG

PLATE 3

A, a longitudinal section, including the surface membrane, of a semitendinosus fibre. Numerous caveolae are located just below the plasmalemma. Necks, where visible, are indicated by arrows. The caveola indicated by the arrow on the left is double. Magnification, × 34,000; calibration = 0·5 μm.

B, the cytoplasmic leaflet (Face *A*) of the plasmalemma is the more darkly shadowed area in the right hand segment of the micrograph. Both membrane particles and caveolar openings can be seen and the latter have been encircled in two cases. The pale area on the top left-hand side is myoplasm. As the fracture entered the myoplasm it passed through several caveolae (see arrows). Notice the relatively smooth nature of the caveolar membrane in contrast to the rest of the plasmalemma. Two caveolae have single particles on the *A* face. Magnification, × 75,000; calibration = 0·2 μm.

PLATE 4

A, the cytoplasmic leaflet (Face *A*) of a sartorius fibre plasma membrane. The fractured caveolar necks appear as circular indentations (30 nm) and three of these are shown by arrows. Notice the numerous membrane particles (7–10 nm). Sarcomere length, 2·6 μm; calibration = 0·1 μm.

B, the external leaflet (Face *B*) of the plasmalemma from a sartorius fibre. On this leaflet the necks appear to be raised circles and three of these are shown with arrows. Notice that the membrane particles are less numerous than they are on Face *B* (Pl. 4 *A*). Sarcomere length, 2·6 μm; calibration = 0·1 μm.

C, the cytoplasmic leaflet (Face *A*) of a semitendinosus fibre stretched to a sarcomere length 4·5 μm. All the caveolae in this area of the fibre appear in the dome configuration. Three domes are indicated by arrows. The smooth nature of the caveolar membrane is obvious, once again in contrast to the non-caveolar membrane. Calibration = 0·1 μm.